

14-3-3ε as an Intracellular Mediator of PGRN/TNFR2 Signaling in Promoting Bone Fracture Healing

Chaopeng He, Yonggang Li, Wenyu Fu, Guiwu Huang, Jingwei Bi, Ryan S. MacLeod, Chuan-ju Liu

Department of Orthopaedics and Rehabilitation, Yale University School of Medicine, New Haven, CT, USA

Disclosure: None

Introduction: Fracture healing is a dynamic process involving inflammation, chondrogenesis, osteogenesis, and remodeling, largely driven by mesenchymal stem cells (MSCs). Although bone possesses intrinsic regenerative capacity, healing is often compromised in aging and osteoporotic populations, emphasizing the need to define molecular regulators of repair. Progranulin (PGRN), a multifunctional growth factor-like protein, has emerged as a critical modulator of bone regeneration. PGRN promotes MSC proliferation, chondrogenic differentiation, and endochondral ossification while suppressing excessive inflammation. Its deficiency has been linked to osteoporosis and delayed fracture repair, highlighting its therapeutic potential. Mechanistically, PGRN exerts its protective effects mainly through tumor necrosis factor receptor 2 (TNFR2), which drives tissue regeneration in contrast to the pro-inflammatory TNFR1 pathway. Our previous work identified 14-3-3ε as a key intracellular mediator of PGRN/TNFR2 signaling, with established roles in arthritis protection and osteogenic differentiation (Tang, et al, *Science*, 2011; Fu, et al, *JCI*, 2021; Fu, et al, *ARD*, 2021). In this study, we utilized 14-3-3ε conditional knockout mice to investigate its role in fracture healing, demonstrating that the PGRN–TNFR2–14-3-3ε axis coordinates chondrogenesis and osteogenesis to ensure optimal repair.

Methods: Single-cell RNA sequencing (scRNA-seq) data from GEO (GSE154247) were analyzed to profile transcriptomic changes during fracture healing. Data preprocessing and downstream analyses, including normalization, clustering, and differential expression, were performed using Seurat, with UMAP visualization for cell-type assignment. For histological assessment, femoral sections were stained with Safranin O/Fast Green to evaluate cartilage matrix integrity. Osteogenic and chondrogenic differentiation of bone marrow-derived MSCs from WT and 14-3-3ε KO mice were assessed by Alizarin Red S and Alcian Blue staining, respectively, with gene expression of lineage markers quantified by qRT-PCR. Micro-CT scanning was performed on fractured femurs at postoperative day 21 to quantify callus architecture and mineralization. Identical reconstruction parameters and thresholding were applied across groups for structural analysis.

Results: 14-3-3ε Expression and Its Role in MSC Chondrogenic and Osteogenic Differentiation. scRNA-seq analysis of fracture site samples (day 14 post-fracture) revealed broad expression of Ywhae (14-3-3ε) across multiple cell types, with notable enrichment in mesenchymal stem cells (MSCs), chondrocytes, and macrophages (Fig. 1A, B). To examine its functional relevance, MSCs isolated from WT and 14-3-3ε KO mice were induced toward chondrogenic and osteogenic lineages. In vitro, WT MSCs exhibited robust glycosaminoglycan deposition by Alcian Blue staining and mineralized nodule formation by Alizarin Red staining, whereas KO MSCs showed markedly reduced cartilage matrix and impaired mineralization (Fig. 1C, D). PGRN treatment further enhanced both chondrogenesis and osteogenesis in WT cells, but failed to rescue these defects in KO MSCs, suggesting that 14-3-3ε is required for PGRN-mediated lineage differentiation (Fig. 1E, F).

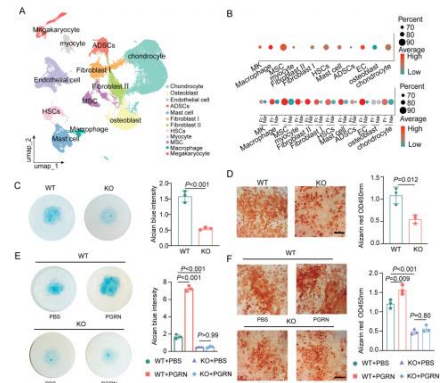


Figure 1. 14-3-3ε Expression and Its Role in MSC Chondrogenic and Osteogenic Differentiation. (A) UMAP visualization of single-cell RNA-seq data identifies distinct cell populations. (B) Dot plot showing expression levels and proportion of cells expressing Ywhae (14-3-3ε) across different cell-type under control and fracture conditions. (C) Alcian blue staining of cell-type (WT and 14-3-3ε^{-/-} KO) hBMSCs following chondrogenic induction. (D) Alizarin Red staining of WT and KO hBMSCs after osteogenic induction. (E) Representative images of Alcian blue staining and quantification of WT and 14-3-3ε^{-/-} hBMSCs under chondrogenic conditions with and without PGRN. (F) Representative images of Alizarin Red staining and quantification of the 10 show mineral deposition with and without PGRN. Data represent mean ± SD. P-values determined by paired two-tailed Student's t-test and one-way ANOVA, n = 3 independent experiments.

14-3-3ε Deficiency Impairs Fracture Healing in vivo.

In a closed femoral fracture model, Safranin O/Fast Green staining at day 22 post-fracture revealed a prominent and persistent cartilaginous callus in KO mice, in contrast to the more advanced ossification and replacement of cartilage by bone tissue observed in WT controls (Fig. 2A, B). Consistently, high-resolution micro-CT confirmed impaired bone regeneration in KO animals, demonstrating incomplete bridging of the fracture gap, markedly lower bone mineral density, and reduced trabecular number, thickness, and connectivity compared with WT counterparts, thereby indicating delayed endochondral ossification and compromised bone healing capacity (Fig. 2C, D).

PGRN accelerates fracture healing in WT mice but not in 14-3-3ε knockout mice.

To test whether PGRN-enhanced regeneration requires 14-3-3ε, WT and KO mice with femoral fractures received either PBS or recombinant PGRN. In WT mice, PGRN treatment

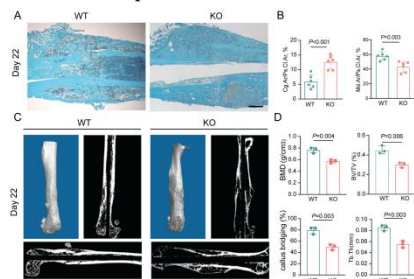


Figure 2. 14-3-3ε Deficiency Impairs Fracture Healing in vivo. (A, B) Representative images of Safranin O/Fast Green staining and quantification of femoral fracture callus sections at day 22 post-fracture in WT and 14-3-3ε^{-/-} mice, n = 6 per group. (C) Micro-CT 3D reconstructions and cross-sectional views of femurs at day 22 post-fracture. (D) Quantification of bone healing parameters at the fracture site, including bone mineral density (BMD), bone volume fraction (BV/TV), callus bridging percentage, and trabecular thickness (Tb.Th), n = 3 per group. Data are presented as mean ± SD. P-values were determined by unpaired two-tailed Student's t-test.

accelerated endochondral ossification, with Safranin O staining showing reduced cartilage retention and Micro-CT demonstrating complete bony bridging and improved bone microarchitecture (Fig. 3A-D). In KO mice, however, PGRN failed to promote cartilage-to-bone transition or enhance bone regeneration, indicating that its pro-healing effects depend on 14-3-3ε signaling.

Conclusion and significance: This study identifies 14-3-3ε as a key intracellular mediator of the PGRN/TNFR2 signaling axis in fracture repair. Loss of 14-3-3ε impaired mesenchymal stem cell chondrogenesis, osteogenesis, and endochondral ossification, resulting in delayed fracture healing. Importantly, recombinant PGRN promoted cartilage and bone formation and accelerated callus maturation in WT mice, but failed to confer benefits in 14-3-3ε-deficient mice, demonstrating that its regenerative effects are critically dependent on 14-3-3ε. Collectively, these findings highlight the PGRN–TNFR2–14-3-3ε axis as an essential regulatory pathway in skeletal repair and a potential therapeutic target to enhance bone regeneration and overcome impaired fracture healing.

Reference: Tang, et al, *Science*. Apr 22 2011;332(6028):478-84. Fu, et al, *J Clin Invest*. Aug 16 2021;131(16). Fu, et al, *Ann Rheum Dis*. Dec 2021;80(12):1615-1627.

Funding: This work was supported partly by NIH research grants R01AR078035, R01AR062207, R01AR076900 and R01NS070328.

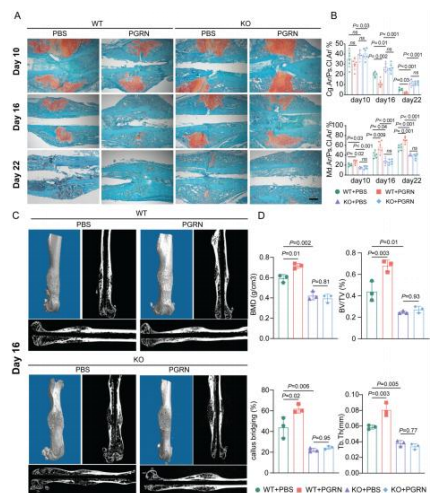


Figure 3. PGRN accelerates fracture healing in WT mice but not in 14-3-3ε knockout mice. (A, B) Safranin O/Fast Green staining and quantification of femoral fracture callus sections at day 10, 16, and 22 post-fracture in WT and 14-3-3ε^{-/-} mice treated with either PBS or PGRN, n = 6 per group. (C) Micro-CT 3D reconstructions and longitudinal sections of fracture calluses at day 16 show bone bridging and mineralization in WT and KO mice treated with either PBS or PGRN. (D) Quantification of Micro-CT bone healing parameters including bone mineral density (BMD), bone volume fraction (BV/TV), callus bridge (%), and trabecular thickness (Tb.Th), n = 3 per group. Data are shown as mean ± SD. P-values were calculated by one-way ANOVA with post hoc analysis.